Velho, J., Santos, N. F., Conceição, S., Ferreira, P. J., Carvalho, M. G., Ferreira, J. M. (2004). Technical aspects for surface, structure and print characterization of coated papers. Proc. *PulPaper 2004*, Helsinquia, Finlândia (versão CD-ROM, 8 pp.).

Technical Aspects Relatively to Surface, Structure and Print Characterization of Coated Papers

José Velho[1], Natércia Santos[2], Susana Conceição[4],
Paulo Ferreira[3], Graça Carvalho[3], José Maria Ferreira[4]
[1]Dep. of Geosciences, University of Aveiro, 3810-193 Aveiro, Portugal. jvelho@clix.pt
[2]Dep. of Chem. and Environmental Eng., Polytechnical Institute of Tomar, 2300 Tomar, naterciasantos@ipt.pt
[3]Dep. of Chemical Eng., University of Coimbra, 3030-290Coimbra, paulo@eq.uc.pt; mgc@eq.uc.pt
[4]Dep. of Ceramics and Glass Eng., Univ. Aveiro, 3810-193 Aveiro. sconceicao@cv.ua.pt; jferreira@cv.ua.pt

ABSTRACT

This paper focuses on the analysis of coated paper properties. The main subject of this paper is to find out ways to define and analyse coated paper properties, namely surface and structure, as well as, in a secondary position, printability. For that, several techniques were used: mercury intrusion porosimetry, scanning electron microscopy, atomic force microscopy and the technique of the contact angle measurements. The papers under study were produced in lab conditions with different coating pigments, such as ground calcium carbonate (GCC), precipitated calcium carbonate (PCC) and kaolin, which were applied in coating colour with different formulations.

The results show the potential of each technique and reveal the advantages of combining the information obtained by each one in order to have a large picture of the coated paper characteristics.

INTRODUCTION

Coated papers have a superior quality in terms of surface and structure, due to the formation of the coated layer. Application of mineral coatings on a paper base is a major goal in order to achieve benefits in terms of paper printability and appearance. The properties of the finished paper sheet depend on the coating formulation (pigments and additives), namely its composition and colour, the application process and the adhesion to the paper base surface. Since the major component of a pigment coating is the pigment *per se*, the evaluation of the paper coated quality requires the study of the particle size distribution, particle shape and packing ability of the pigment, which affect the porosity and the pore structure of the coating layer [1] [2] [3].

Therefore, it is expected that the use of distinct pigments in the coating colour formulation, such as GCC (ground calcium carbonate), PCC (precipitated calcium carbonate) and kaolin, having different intrinsic characteristics, are responsible for coating layers with different properties and also for papers with distinct printability and optical characteristics. At present, there is a general trend to develop new techniques and to find out new indexes in order to characterize the sheet surface and structure and to establish relationships between these parameters and coating formulation and printability.

The main goal of this work is to show the potential of using simultaneously different techniques in order to analyse paper coated properties, namely surface and structure, as well as printability. Mercury intrusion porosimetry, scanning electron microscopy (SEM), atomic force microscopy (AFM) and surface energy and the technique of the contact angle measurement are analysed using several examples.

MERCURY INTRUSION POROSIMETRY

Mercury intrusion porosimetry is based on the capillarity law that governs the penetration of liquids in pores of small dimensions. This law is expressed by Washburn equation:

$$D = -(1/P)\, 4\, \gamma \cos \varphi$$

where D is the pore diameter, P is the applied pressure, γ is the surface tension and φ is the contact angle.

According to this theory, the pores are considered as cylinders. Although this fact is not really true for paper webs and paper coating layers, it is generally accepted because it is a practical way to evaluate their porous structure.

The mercury volume, V, which penetrates into the pores, is measured directly as a function of the applied pressure. The mercury surface tension, although changing with its purity, is assumed to be equal to 485 dynes/cm, whereas the contact angle between the mercury and the pore solid is considered equal to 130º.

In this work, for the pore structure determinations of both mineral filler and paper sheets, mercury intrusion porosimetry was chosen and the Poresizer 9320 apparatus from Micromeritics was used. The advance of contact angle was 137º, the average sample weight 0,321 g, the equilibration time 20 sec. and the maximum intrusion volume 0,0500 mL/g. The following pore structure parameters were assessed: total intrusion volume (in mL/g), total pore area (in m^2/g), average pore diameter (in μm), apparent density (in g/mL) and intrusion porosity (in %).

Coating structure analysis

One of the most important problems in terms of paper coating is the accurate knowledge of the coating layer structure. Mercury intrusion porosimetry is very useful because one can estimate the porous volume and the pore size distribution of the coating layer besides other important parameters. The volume of pores of the coating layer is obtained from the volume of pores in the range of 1-0,1 μm of the coated paper minus the volume of pores in the range of 1-0,1 μm of the base paper. Although this assumption do not reflect exactly the phenomenon,

because calendering exerts a certain influence on pore size distribution, the results obtained for different coated papers with different pigments are very interesting and are very useful, providing good correlations between the pore structure and the optical properties (like light scattering coefficient).

Figure 1 shows the pore size distribution of two coated papers and the corresponding base paper. The coated papers were prepared in laboratory by coating the base paper (an offset paper having a basis weight of $100 g/m^2$) on one side. Coating weight on each side was 15 g/m^2.

Comparing the pore size range between 0,1-1 μm it is visible that the coated layer of pigment E is much more porous than the coated layer of pigment G. This is due to the fact that pigment E has a bulky nature, related to its scalenohedral tendency to pack in clusters, whereas pigment G tend to form a more compact structure, because its particles are predominantly round shaped.
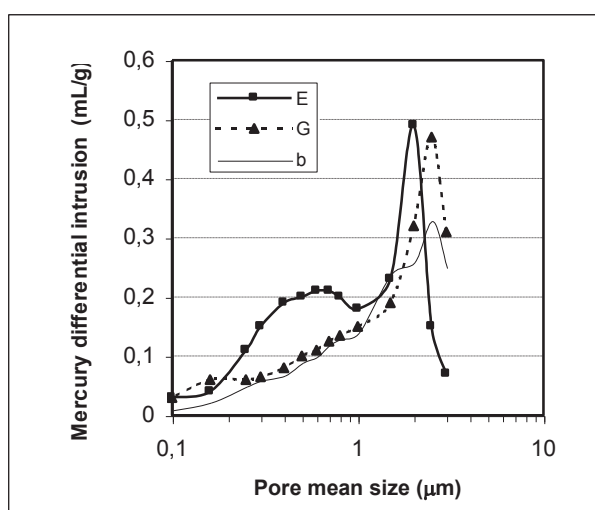

Fig. 1. Pore size distribution of coated papers and base paper: E – coated paper with PCC as pigment (scalenohedral particle shape); G – coated paper with GCC as pigment; b – base paper.

Figure 2 shows that the optical ability of the coated papers is related with its coating pore volume: the light scattering coefficient of the coated papers increases with the increment of the pore volume of the coated layer.

This analysis is very important because it shows that it is possible to optimise the optical properties of coated papers (for example, if light scattering is a critical property) by adjusting the pigment formulation in order to control the pore volume of the coated layer.

Roughness

Mercury intrusion porosimetry can also be applied for the roughness (micro-roughness) evaluation of the coated papers, which is an important parameter that controls sheet gloss. There are several methods to assess paper roughness but the correlation between them is poor.

Figure 3 shows a very good agreement between the RZI roughness index and the mercury intruded volume at the surface. The results refer to a coated paper with kaolin as pigment and with a coating basis weight of about 2,5 g/m^2. The base paper has a surface pore volume of about 0,0117 mL/g for a class of pores ranging between 7 μm and 15 μm (measured by mercury intrusion porosimetry). Surface pore volume is the difference between intruded mercury volume of coated paper and base paper for pore sizes ranging between 7 μm and 15 μm.
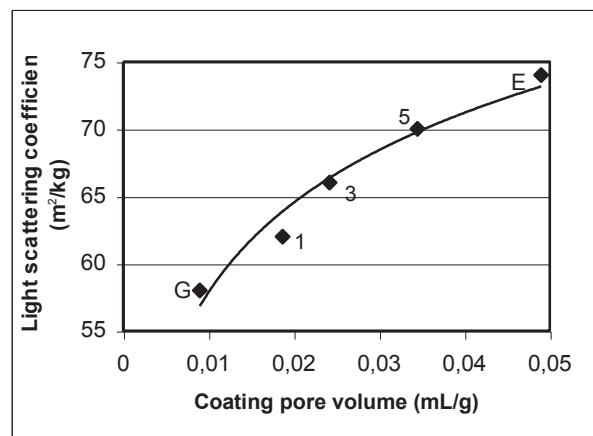

Fig. 2. Light scattering coefficient as a function of coating pore volume. Coated papers with different proportions of pigments E and G in the coating formulation: G-GCC100; 1-GCC75:PCC25; 3-GCC50:PCC50; 5-GCC25:PCC75; E–PCC100.

The RZI index is a function of the Rz roughness index (measured in a mechanical roughmeter, as the Perthometer S4P, Perthen used in this work): $RZI=[(Rz_{MD})^2+(Rz_{CD})^2]^{1/2}$. This index takes into account the contribution of the topographic parameter Rz from MD and CD to the overall paper roughness.
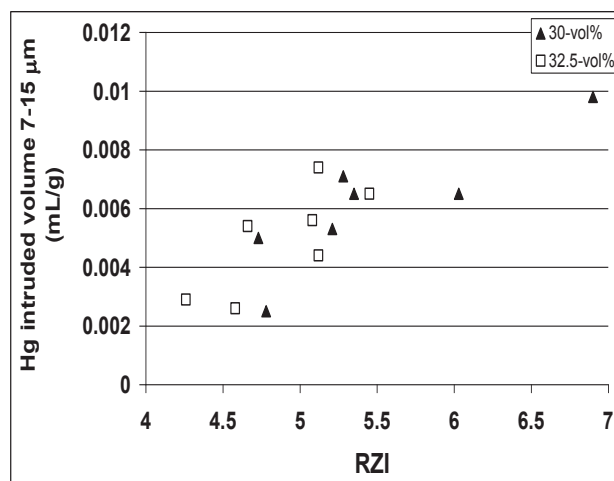

Fig. 3. Relationship between RZI and surface porosity measured by mercury intrusion porosimetry.

Several coating colour formulations were obtained with two different solid concentrations (30-vol% and 32.5-vol%) and with two different rheological modifiers (CMC35, having a molecular weight of 35,000g/mol, and CMC250, having a molecular weight of 250,000g/mol). These modifiers have been added separately and mixed in a 1:1 ratio, in total amounts of 0.1-wt.% and 0.2-wt.% relative to dry mass of kaolin. The coating colour formulations also included 10 parts of carboxylated styrene-butadiene latex and 1 part of acrosol (acrylester copolymer basis) for each part of kaolin.

Sheet gloss

It is very difficult to analyse the sheet gloss because it is influenced by the sheet surface roughness in different scales. Sheet roughness is usually evaluated at different levels (macro, micro and nano-roughness), in order to get a general vision of sheet surface. As mentioned before, mercury intrusion porosimetry only supplies the measurement of the micro-roughness.

The contribution of mercury intrusion porosimetry in providing correlations between surface porosity (micro-roughness) and sheet gloss is presented in figure 4.
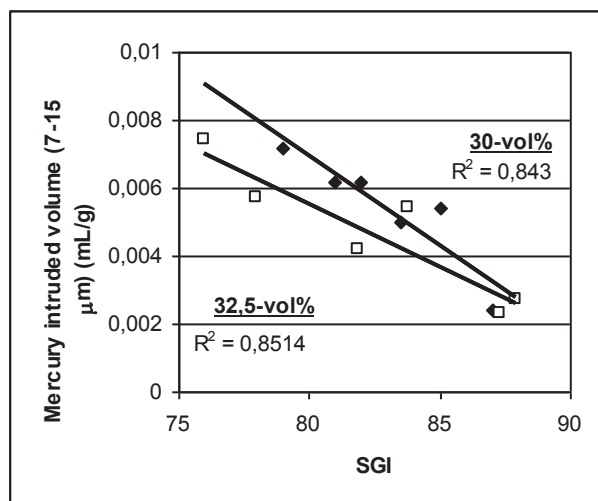
Fig. 4. Relationship between SGI and surface porosity for coating colours with kaolin.

This figure shows the inverse relationship between sheet gloss index SGI and the difference between the intruded volume of mercury of the base and of the coated papers, in the pore diameter range of 7 μm to 15 μm.

SGI is an index that takes into account the contribution of the sheet gloss measured in the MD and in the CD directions to the overall sheet gloss (SG), and is computed as: $SGI=[(SG_{MD})^2 + (SG_{CD})^2]^{1/2}$. The main goal of this index is to combine measurements that are dependent of a certain direction in a new value that can be representative of the whole surface. Thus, it is possible to compare SGI with other properties such as the mercury intrusion properties.

Rheology

Coated paper properties, such as coating thickness and structure, which in turn determine the optical properties of the coated paper, are closely related to the specific morphological features of the pigment present in the coating colour formulation and to the specific interactions between the pigment and the polymeric chains of the rheological modifiers and co-binders. These molecular interactions determine the configuration of the adsorbed polymeric chains that depend on the molecular weight of the rheological modifiers.

A close interaction between the rheology of the coating colours and the properties of the coated paper is found.

Figure 5 presents the light scattering coefficient as a function of the shear stress of the coating colours measured at a shear rate of 1250 s^{-1}. The pigment in the coating formulation is kaolin at two concentration levels (30-vol% and 32.5-vol%) and the rheological modifiers are CMC35 and CMC250 at 0,2 (vol%). For all the CMC formulations tested, an inverse relationship between shear stress and light scattering coefficient is detected.
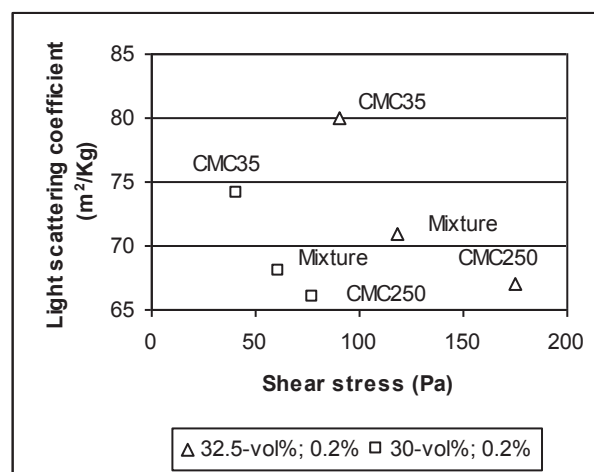
Fig. 5. Light scattering coefficient as a function of the shear stress (mixture=CMC35+CMC250 in a 1:1 ratio).

CMC molecules have a tendency to remain in the solution rather than to be adsorbed at the particles surface, due to particle shape and, specially, to the particle charge surface distribution of kaolinite.

The situation is quite different for GCC particles, which are round-shaped – polymeric CMC chains may form different configurations upon adsorbing onto the GCC particles surface. On the one hand, a more airy-like conformation would be expected for the low CMC35, while the longer CMC250 chains would probably adsorb through several segments forming loops and less extended tails to the solution. In fact, the solvency of CMCs in water is improved as the molecular weight decreases. On the other hand, the thickness of the adsorbed layers, the relative affinity of the adsorbing species to the surface, their solvency in the media and the

adsorbed amount are all strongly interrelated. For instance, at 0,1-wt.% CMC35, the polymeric chains might be able to bend and partially align according to the flow direction. Increasing the amount of CMC to 0,2-wt.% would lead to a higher degree of surface coverage and a denser adsorbed layer.

As for the longer polymeric chains of the CMC250, they may adsorb at the surface of different neighbouring particles, especially under a low degree of surface coverage (0.1-wt.% CMC250), thus promoting bridging flocculation. Increasing the amount of CMC250 to 0.2-wt.% will enhance the surface coverage and reduce the probability of one polymeric chain to adsorb in more than one particle, therefore decreasing the trend for bridging flocculation.

Since these different interactions influence the pigment packing ability, it would be expected that mercury intrusion porosimetry could give useful information regarding the effect of the co-binders. Data in table 1 refer to six different coating colours formulations with GCC at 50-vol% concentration level.

Table 1. Results for coated papers with GCC (50-vol%)

Porosimetric parameters	CMC35 0,2-wt%	Mixture 0,2-wt%	CMC250 0,2-wt%
Total intrusion volume (mL/g)	0,4172	0,4599	0,4065
Total pore area (m^2/g)	6,840	6,003	5,760
Median pore diameter (μm)	1,7966	2,1170	1,8403
Average pore diameter (μm)	0,2440	0,2626	0,2823
Porosity (%)	42,53	44,21	40,86
Bulk density (g/mL)	1,0192	0,9613	1,0052

As can be seen from the total pore area results, with CMC35 the structure of the coating layer is responsible for finer pores than with CMC250. As for CMC250, due to its dominant role for bridging flocculation, the corresponding papers have low values of mercury intrusion volume as well as pore area. As a consequence, papers with CMC35 have higher values of light scattering than papers with CMC250.

SCANNING ELECTRON MICROSCOPY (SEM)

SEM roughness index (SRI), which is based on the standard deviation of colours spectrum, is obtained with SEM observations of coated paper surfaces in special conditions [4]. A perfect surface, with a 100% sheet gloss, is assumed to have a standard deviation equal to zero. This index is very sensitive to coated papers with different pigments.

Figure 6 shows the relationship between SRI and sheet gloss, considering distinct calendaring levels, coating pigments and formulations. Points refer to coated papers with GCC and PCC pigments, and fit very well with the so called perfect paper surface: coated papers with GCC have a very low standard deviation value, meaning that the paper surface is not so irregular and so paper is glossy. Between the 1st and the 2nd calendaring stages two individual trends can be identified, both having high

correlation index values (with the one that corresponds to the 2nd stage showing higher gloss values). This clear indicates that for the same standard deviation level, the 2nd stage gives a glosser paper.
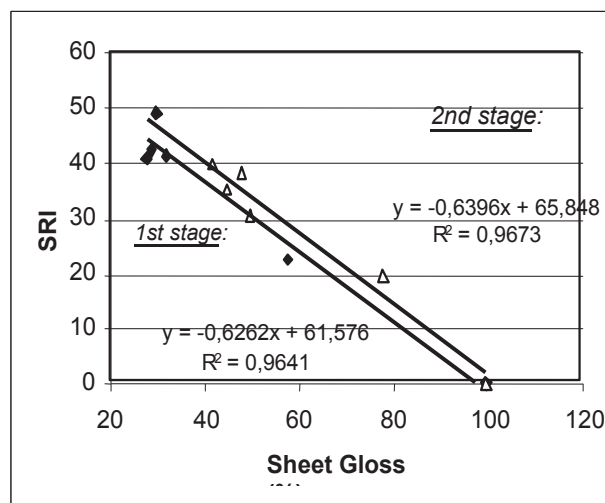

Fig. 6. Sheet gloss vs. SRI in function of calendering.

Figures 7 and 8 refer to papers coated with kaolin, the coating formulation having now solids content (30-vol% and 32.5-vol%) and rheological modifier (type and concentration). Figure 7 reveals a logical and positive correlation between surface porosity (measured by mercury intrusion porosimetry) and SRI. Figure 8 relates SRI and RZI indexes. There is also a positive trend but in both situations (figs. 7 and 8), there is coincident the evolution between 30-vol% and 32.5-vol%.
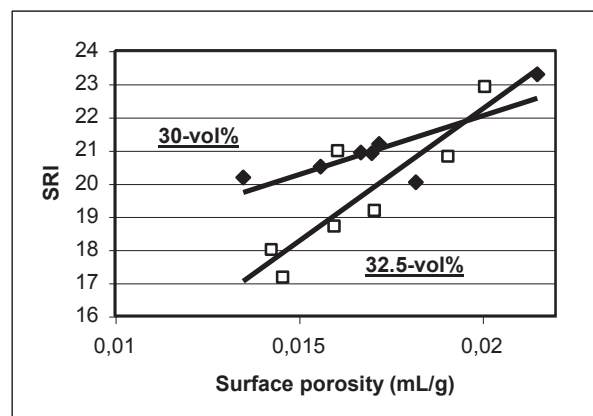

Fig. 7. Surface porosity vs. SRI for coated papers with kaolin.

RZI and SRI indexes characterize the roughness of the sheet surface at a micro scale level, and it is thus expected that good correlations with measurements performed at a macro scale level, as those obtained by the Bendtsen technique, are difficult to achieve. This is confirmed by the results depicted in figures 9 and 10.
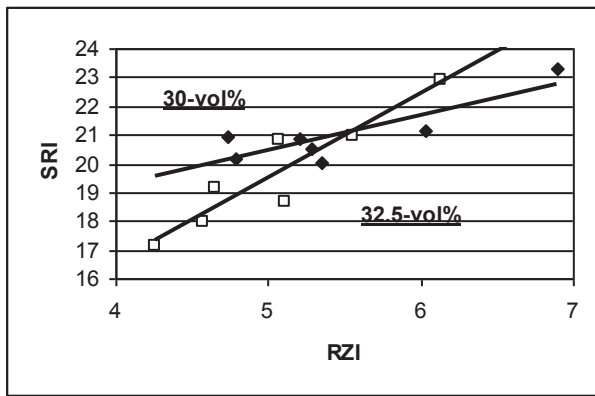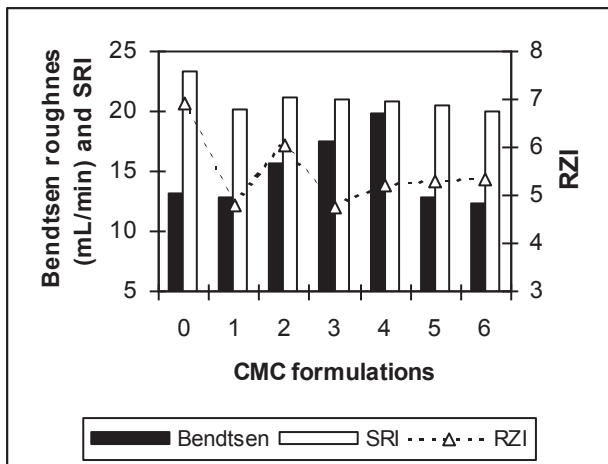
Fig. 8. SRI vs. RZI for coated papers with kaolin.

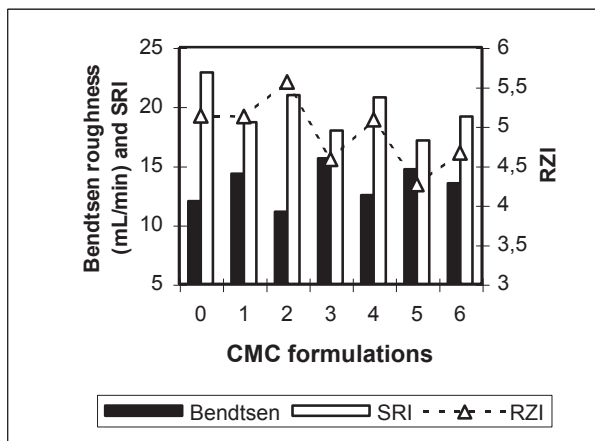**Fig. 9.** Roughness results of coated papers with kaolin (30-vol%).

Fig. 10. Roughness results of coated papers with kaolin (32.5-vol%).

ATOMIC FORCE MICROSCOPY (AFM)

The AFM measured 10 μm square spot sizes. Measurements were done using a "Multimode" Nanoscope III A in a tapping mode OTESPA (Olympus, 330 kHz, spring constant 42 N/m).

RMS roughness

The mode used in AFM consisted in a non contact tapping one; the probe tip is oscillated above the surface such that the amplitude of the oscillation is influenced by the proximity to the surface.

The sample is moved vertically to maintain constant oscillation amplitude, providing topographic information. With AFM a topographic map was provided and several statistics were calculated using appropriate software. Table 2 show RMS roughness results of coated papers with ground calcium carbonate and precipitated calcium carbonate and respective blend formulations, when subjected to two calendering stages, 2x and 4x.

Table 2. RMS Roughness (nm) results

	G	1	3	5	E
2x	68	148	152	110	161
4x	42	74	132	82	66

The results show the influence of calendering on sheet topography especially on E formulation as well as the packing difficulty of formulation 3. G formulation is the one that has the lowest roughness values.

Another way to apply AFM is to analyse paper surface roughness in print/non print zones in function of calendering stages. Figure 11 show RMS results of coated papers with a precipitated calcium carbonate pigment with scalenohedral particle shape. This pigment is present in a coating colour formulation with a solid content of 30-vol%. As rheological modifier, a mixture CMC35: CMC250 in a ratio 1:1 (in total amount of 0.1-wt.% relative to dry mass of precipitated calcium carbonate) was selected. This coated paper was subjected to different calendering stages (0, 1 and 2 times) and was printed in a laser printer.
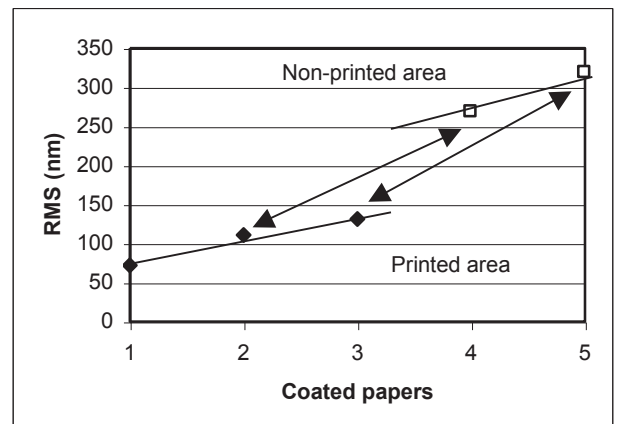
1-Calendering stage – 2x and printed area;
2-Calendering stage – 1x and printed area;
3-Non calendered paper and printed area;
4-Calendering stage – 1x and non-printed area;
5-Non calendered paper and non-printed area.

Fig. 11. RMS results for coated papers.

Printed areas are smoother and this smoothness is directly proportional to calendering level. AFM proved to be very sensitive in terms of evaluation between printed and non-printed areas.

It is also possible to find out an interesting correlation between RMS of printed areas and print gloss. For calendered level 1x, RMS is 110.86 nm. The respective values of print gloss are: 65.0 (CD) and 58.1 (MD). For calendered level 2x, RMS is 71.97 nm and print gloss is: 72.4 (CD) and 65.4 (MD).

Topography

Choosing a certain "water level", it is possible to count the number of islands that are above the water surface, as well as the correspondent flooding volume. For example, if one selects a 50% flooded area level, it means that half of surface area is flooded. Then, it is possible to register the number of islands as well as the total flooded volume correspondent to a 100% flooding. The methodology used was using this flooding technique for a 25%, 50% and 75% flooded area. For each one, the numbers of islands and the correspondent flooded volume were evaluated. For each flooded area the index *number of islands/total flooded volume* was calculated. Each sheet surface is characterized by three values that reflect in somewhat sheet topography. Using them one can evaluate a steepness index:

$$SI=[(top_{75}-top_{25})/top_{50}]$$

where, SI is the steepness index, top_x is the topography defined by the index identified above relatively to different flooded area values.

We consider a glossy surface the one that shows a higher number of islands relatively to the total flooded volume as well as has a narrow distribution of topographic irregularities. Table 3 shows the results obtained for coated papers with ground and precipitated calcium carbonate pigments for a 50% flooded area.

Table 3. AFM results for a 50% flooded area

Pigments	G		E	
Calendering levels	2x	4x	2x	4x
Flooding (%)	50	50	50	50
Number of islands	68	86	75	65
Total volume (μm^3)	4,34	2,72	12,26	3,52
Sheet gloss (%)	58	78	31	52

For the same flooded area, paper with G pigment show lower total flooded volume than with E pigment. For the last one, between 2 and 4 calendering levels, there was a great decrease on total flooded volume (about 71%), the surface became smoother, with lesser irregularities and the number of islands also decreased (from 75 to 65). For G pigment, total flooded volume also decreased, but in a lesser amplitude than for E (about 37%) but the number of islands increased from 68 to 86. E pigment particles occur in soft and flexible aggregates, so, they respond actively to calendering. G pigment particles show a high

packing ability, those particles occur individually, so, calendering is not so efficient in terms of flooded volume reduction.

Sheet gloss is dependent on surface roughness and total flooded volume as well as on the uniformity of the paper surface, it means on the number of islands.

Figure 12 shows the relationship between sheet gloss and the steepness index measured from flooding technique taking into account different flooded area values, 25%, 50% and 75%. In this situation, the results are referred to papers calendered 2x. In a similar way that was presented in figure 11, SI results can be compared between each other in function of coated papers.

Figure 13 shows SI results of coated papers with precipitated calcium carbonate as pigment with a solid content of 30-vol% in the coating colour formulation.

Fig. 12. Steepness index (SI) vs. sheet gloss (%).

Figure 13 shows SI results of coated papers with precipitated calcium carbonate as pigment with a solid content of 30-vol% in the coating colour formulation.
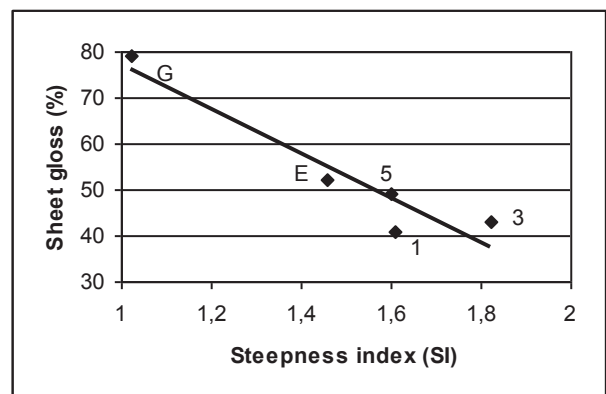

1-Calendering stage – 2x and printed area;
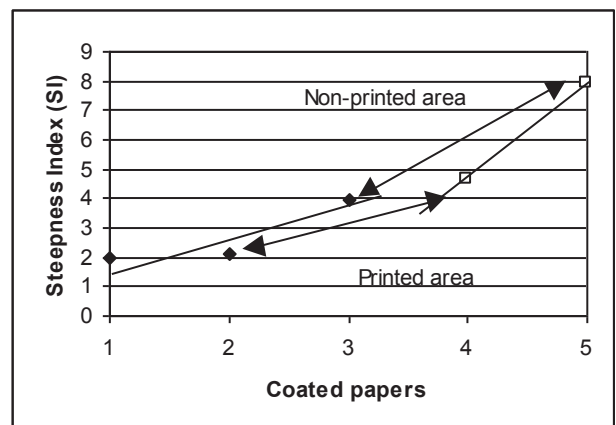2-Calendering stage – 1x and printed area;
3-Non calendered paper and printed area;
4-Calendering stage – 1x and non-printed area;
5-Non calendered paper and non-printed area.

Fig. 13. Steepness Index results for coated papers.

CONTACT ANGLE AND SURFACE ENERGY

Dispersive components

The paper printing process is based on interactions between liquids (inks) and solids (paper surface). Due to different types of interactions, surface tension (or surface free energy) can be divided into dispersive and polar components:

$$\sigma_l = \sigma_l^d + \sigma_l^p; \; \sigma_s = \sigma_s^d + \sigma_s^p$$

where σ_l^d and σ_l^p represent the dispersive and polar parts of the surface tension of the liquid, while σ_s^d and σ_s^p represent the respective contributions to the surface energy of the solid. The interfacial energy (σ_{sl}) of the newly formed interface can be calculated according to Owens, Wendt, Rabel and Kaelble (OWRK method) from the contributions of the liquid and the solid surface energies and their dispersive and polar parts by forming a geometric mean. For σ_{sl} one obtains:

$$\sigma_{sl} = \sigma_s + \sigma_l - 2((\sigma_s^d \cdot \sigma_l^d)^{0,5} + (\sigma_s^p \cdot \sigma_l^p)^{0,5}$$

Using the Young equation, $\sigma_s = \sigma_{sl} + \sigma_l \cos\theta$, and solving for the unknown quantities, an equation of a straight line is obtained, in the form:

$$y = a \cdot x + b.$$

By plotting y $((1+\cos\theta)/2 \cdot (\sigma_l/(\sigma_l^d)^{0,5}))$ versus x $((\sigma_l^p/\sigma_l^d)^{0,5})$, σ_s^p and σ_s^d can be calculated from the slope of the fitted line and from the intersection with the vertical axis, respectively. To achieve this, the contact angle of at least two liquids with the unknown solid must be determined. The contact angle measurements were performed on the equipment OCA20 from DataPhysics. Table 4, gives a list of liquids that were used for the contact angle measurements, along with the values of their surface energy and dispersive and polar components.

Table 4. Experimental values of the surface tension and its components of the liquids used (mN/m)

Liquid	Surface energy	Dispersive component	Polar component
Water	72,78±0,08	24,73±0,12	48,05±0,14
Ethylene glycol	48,28±0,04	30,93±0,07	17,35±0,08
Formamide	58,13±0,05	32,28±0,07	25,85±0,09
Propylene glycol	35,4±0,10	26,4±0,20	9,0±0,20

Surface energy

For surface energy determinations of coated papers, three sets were selected, each one with different pigment: kaolin and PCC (with scalenohedral particle shape) in a 20:80 ratio (K+PCC), PCC with scalenohedral particle shape but with different particle size distribution (PCC-1) and PCC with acicular particle shape-aragonite (PCC-2).

In each set, different coating colour formulations were selected, based on the type of co-binder: CMC (35, 250 and 35:250 in a 1:1 ratio), HEC and MHPC, all of them present in a concentration of 0,1-wt%. Solids content were as follows: K+PCC: 35-vol%; PCC1: 50-vol% and PCC2: 48-vol%. Coating grammage has varied between 2,2 g/m^2 and 3,4 g/m^2. The results are listed in table 5.

The results show that it is possible to produce coated papers with different values of surface tension by changing the type of pigment, solids content and co-binder formulation. Despite the fact that the first set is responsible for papers with lower surface tension values, their polar components are very high. Papers with PCC-1 show a higher surface tension and disperse component (with a lower polar component) than with PCC-2. The reasons why there is such great difference between the paper properties with these two PCC pigments lye in the chemical additives present during the synthesis process.

The sequence between CMC35 and CMC250 are very interesting. For K+PCC formulation, there is an increase, in terms of polar component, between those two co-binder formulations. But, for PCC-2 formulation, is exactly the opposite.

New co-binders HEC and MHPC gave also interesting results: while the former is responsible for paper surface with low polar component, the latter gives ~~is~~ exactly the opposite.

Table 5. Surface energy of the coated papers (mN/m)

Coating formulation	Surface energy	Disperse component	Polar component
K+PCC coating formulation			
CMC35	22,13	16,51	5,61
CMC35+CMC250	21,31	12,48	8,83
CMC250	22,44	12,69	9,75
PCC-1 formulation			
No co binder	24,53	22,88	1,66
CMC35	22,66	25,20	1,46
CMC35+CMC250	23,32	20,46	2,86
CMC250	24,07	21,80	2,27
HEC	27,42	26,02	1,41
MHPC	27,29	19,23	8,06
PCC-2 formulation			
No co binder	22,74	19,12	3,62
CMC35	22,89	17,36	5,53
CMC35+CMC250	24,69	19,65	5,04
CMC250	25,30	21,66	3,64
HEC	23,61	18,62	4,99
MHPC	23,59	16,22	7,37

One coloured printing ink (yellow) and black printing ink, both extracted from HP560C cartridge, were also selected for surface tension measurement. In table 6 the surface tension values as well as their dispersed and polar parts are given.

The differences between the yellow and the black ink are very clear: in contact with a paper sheet, the former is expected to give a lower contact angle and a higher spreading and penetration rate than black ink. Probably, for inkjet printing with black ink, paper surface with a low polar component will be preferable. For yellow ink, due to its great disperse behaviour, and in order to avoid feathering, probably paper surface with high polar component will be suitable for a better printability.

Table 6. Surface tension of printing inks (HP560C).

Liquid	Surface energy	Dispersive component	Polar component
Black	42,47±0,01	30,91±0,02	11,56±0,02
Yellow	31,59±0,04	30,78±0,05	0,81±0,02

Contact angle

Table 7 shows the contact angle of various polar liquids with the coated papers. The presence of co-binders in coating colours formulations makes the paper surface less hydrophobic. MHPC, in general trend, shows the lowest contact angle while HEC behaves similar of that of CMC35.

The results show that it is possible to obtain different contact angles varying coating colour formulations and, especially, mineral pigment. The best relationship between polar component and the contact angle is observed using water (as Figure 14 shows) followed by formamide, ethylene glycol and propylene glycol. It means that the correlation index decreases with the decrease of the polar component of the liquid surface tension.

Table 7. Contact angles (degree) between papers and various liquids for different coating colour formulations

Coating formulation	Contact angle (θ)			
	Water	Ethylene glycol	Forma-mide	Propylene glycol
K+PCC formulation				
CMC35	89,2	71,0	76,4	50,5
CMC35+CMC250	86,6	72,1	76,9	49,0
CMC250	84,9	71,2	73,7	48,9
PCC-1 formulation				
No co binder	95,7	71,5	80,4	52,1
CMC35	95,5	70,6	76,0	47,3
CMC35+CMC250	93,6	70,8	77,5	53,2
CMC250	94,4	71,8	78,7	51,3
HEC	93,6	70,8	75,8	47,1
MHPC	79,9	62,3	67,3	39,7
PCC-2 formulation				
No co binder	93,0	69,5	75,4	53,9
CMC35	89,6	65,5	73,4	51,3
CMC35+CMC250	88,0	64,0	73,4	48,5
CMC250	90,3	64,9	73,4	48,3
HEC	89,4	66,4	73,3	50,6
MHPC	86,5	65,5	70,9	50,4

CONCLUSIONS

The results presented in this research and the respective techniques show that there is an enormous field of interest in looking for new applications of known techniques. One of the main difficulties is to deal with such different information, put them together and take conclusions about the optimisation of coated paper, in terms of surface and structure, for the improvement of print quality.
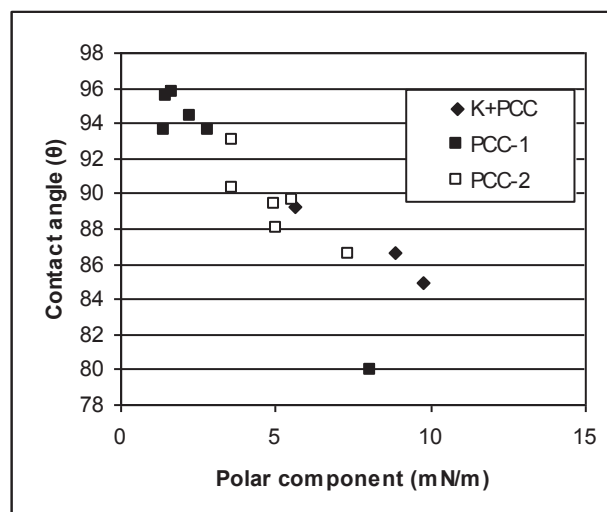
Fig. 14. Relationship between contact angle (with water) and polar component of the surface energy of coated papers.

The results put an emphasis on how different pigments can influence paper properties and, especially, the role of co-binders, CMC, HEC and MHPC.

Contact angle and surface energy determinations showed the great potential of this technique in order to improve paper properties (by changing coating colour formulations) in terms of printability. In fact, for a complete analysis, it will be necessary to use printing tests, with black and coloured inks, to know what are the best formulations and pigments.

REFERENCES
1. Andersson, L.: Some Principles of Coating Formulation. In: Paper Coating Additives, Tappi Press, Atlanta, 1995.
2. Beazley, K.: Surface Coating. In Pira Reviews of Pulp and Paper Technology, Pira International, Surrey, 1993.
3. Engstrom, G. and Rigdahl, M.: The Use of some PCC Grades as Coating Pigments. Nordic Pulp and Paper Research Journal 7(1992):2, 55-63.
4. Velho, J., Conceição, S., Santos, N.: A porosimetria de intrusão de mercúrio no estudo de papéis revestidos. Pasta e Papel (in press).